

# Green Chemistry

Accepted Manuscript



This is an *Accepted Manuscript*, which has been through the Royal Society of Chemistry peer review process and has been accepted for publication.

*Accepted Manuscripts* are published online shortly after acceptance, before technical editing, formatting and proof reading. Using this free service, authors can make their results available to the community, in citable form, before we publish the edited article. We will replace this *Accepted Manuscript* with the edited and formatted *Advance Article* as soon as it is available.

You can find more information about *Accepted Manuscripts* in the [Information for Authors](#).

Please note that technical editing may introduce minor changes to the text and/or graphics, which may alter content. The journal's standard [Terms & Conditions](#) and the [Ethical guidelines](#) still apply. In no event shall the Royal Society of Chemistry be held responsible for any errors or omissions in this *Accepted Manuscript* or any consequences arising from the use of any information it contains.



[www.rsc.org/greenchem](http://www.rsc.org/greenchem)

1 **Simultaneous Conversion of All Cell Wall Components by Oleaginous Fungus without**  
2 **Chemi-physical Pretreatment**

3 Shangxian Xie<sup>ab</sup>, Xing Qin<sup>b</sup>, Yanbing Cheng<sup>b</sup>, Dhrubojyoti Laskar<sup>c</sup>, Weichuan Qiao<sup>b</sup>, Su Sun<sup>b</sup>,  
4 Luis H. Reyes<sup>d</sup>, Xin Wang<sup>b</sup>, Susie Y. Dai<sup>e</sup>, Scott E. Sattler<sup>f</sup>, Katy Kao<sup>d</sup>, Bin Yang<sup>c</sup>, Xiaoyu  
5 Zhan<sup>a,\*</sup>, and Joshua S. Yuan<sup>ab,\*</sup>

6 <sup>a</sup> School of Life Science & Technology, Huazhong University of Science and Technology,  
7 Wuhan, 430074, P.R. China

8 <sup>b</sup> Synthetic and Systems Biology Innovation Hub, Department of Plant Pathology and  
9 Microbiology, Institute for Plant Genomics and Biotechnology, Texas A & M University,  
10 College Station, TX, 77843, USA

11 <sup>c</sup> Center for Bioproducts and Bioenergy, Washington State University, Richland, WA, 99354,  
12 USA

13 <sup>d</sup> Department of Chemical Engineering, Texas A&M University, College Station, TX, 77843,  
14 USA

15 <sup>e</sup> Office of Texas State Chemist, Texas AgriLife Research, College Station, TX 77843, USA  
16 Grain,

17 <sup>f</sup> Grain, Forage, and Bioenergy Research Unit, USDA-ARS, Lincoln, NE, 68583, USA

18 \* To whom correspondence should be addressed: Joshua Yuan: [syuan@tamu.edu](mailto:syuan@tamu.edu) and Xiaoyu  
19 Zhang: [zhangxiaoyu@mail.hust.edu.cn](mailto:zhangxiaoyu@mail.hust.edu.cn);

20

21

22

## 23 Abstract

24 Lignin utilization during biomass conversion has been a major challenge for lignocellulosic  
25 biofuel. In particular, the conversion of lignin along with carbohydrate for fungible fuels and  
26 chemicals will both improve the overall carbon efficiency and reduce the need for chemical  
27 pretreatments. However, few biomass-converting microorganisms have the capacity to degrade  
28 all cell wall components including lignin, cellulose, and hemicellulose. We hereby evaluated a  
29 unique oleaginous fungus strain *Cunninghamella echinulata* FR3 for its capacity to degrade  
30 lignin during biomass conversion to lipid, and the potential to carry out consolidated  
31 fermentation without chemical pretreatment, especially when combined with sorghum (*Sorghum*  
32 *bicolor*) *bmr* mutants with reduced lignin content. The study clearly showed that lignin was  
33 consumed together with carbohydrate during biomass conversion for all sorghum samples, which  
34 indicates this organism has the potential for biomass conversion without chemical pretreatment.  
35 Even though dilute acid pretreatment of biomass resulted in more weight loss during fungal  
36 fermentation than untreated biomass, the lipid yields were comparable for untreated *bmr6/bmr12*  
37 double mutant and dilute acid-pretreated wild-type biomass samples. The mechanisms for lignin  
38 degradation in oleaginous fungi were further elucidated through transcriptomics and chemical  
39 analysis. The studies showed that in *C. echinulata* FR3, Fenton Reaction may play an important  
40 role in lignin degradation. This discovery is among the first to show that a mechanism for lignin  
41 degradation similar to ones found in white and brown rot basidiomycetous fungi exists in an  
42 oleaginous fungus. This study suggests that oleaginous fungus such as *C. echinulata* FR3 can be  
43 employed for complete biomass utilization in a consolidated platform without chemical  
44 pretreatment, or can be used to convert lignin waste into lipids.

45

46

## 47 Introduction

48 Lignin modification and utilization are essential for sustainable and cost-effective production  
49 of fuels and chemicals from lignocellulosic biomass. Traditional approach for biomass  
50 conversion follows three steps including pretreatment, saccharification, and fermentation<sup>1, 2</sup> A  
51 major goal of pretreatment is to disrupt lignin structure to make cellulose more accessible to  
52 saccharification.<sup>1, 3</sup> However, most of chemical or physical pretreatment strategies require high  
53 energy input and harsh conditions such as high temperature and/or extreme pH, which often also  
54 resulted in toxic waste. Biological pretreatment, on the other side, can be carried out in milder  
55 conditions and be more environmentally friendly. However, it is still challenging to apply  
56 biological pretreatment for biofuel production due to the long reaction time. Lignin modification  
57 on feedstock thus emerged as an alternative strategy for reducing recalcitrance and developing  
58 cost-effective bioconversion with simplified pretreatment.<sup>4, 5</sup>

59 Traditionally, lignin modification was extensively studied in model plants such as *Medicago*,  
60 *Arabidopsis*, and *Nicotiana*.<sup>4, 6, 7</sup> Recently, significant advances have been made in the  
61 improvement of grasses, including sorghum and switchgrass, as biofuel feedstocks.<sup>8-10</sup> However,  
62 most research on the lignin modification of grasses has been carried out via genetic modification,  
63 which creates regulatory issues for commercial implementation. In contrast, a unique set of  
64 chemically mutagenized lignin modification *brown midrib (bmr)* mutants were developed in  
65 sorghum as major assets in determining how modifications to the lignin biosynthesis pathway  
66 impact biomass conversion.<sup>11, 12</sup> The biomass from *bmr6* or *bmr12* plants was significantly  
67 reduced in lignin content and altered in lignin composition in relative to wild-type biomass. Each  
68 mutant showed increased saccharification and ethanol conversion efficiency for cellulose.<sup>13</sup>  
69 When combined in a double mutant, the effects were additive for reducing lignin content and

70 increasing conversion efficiency.<sup>14</sup> Despite the previous advances in ethanol platforms, few  
71 studies focused on how lignin modification will impact the oleaginous fungus conversion of  
72 biomass into lipid. Also unknown was whether feedstock lignin modification could promote *C.*  
73 *echinulata* FR3 conversion of biomass without chemi-physical pretreatment.

74 Recently, lipid production from biomass using oleaginous microbe has been explored.<sup>15, 16</sup>  
75 Many studies have reported oleaginous fungi, including *Mortierella isabellina* and *Mucor*  
76 *circinelloides*, could produce lipid from lignocellulolytic hydrolysates.<sup>15, 16</sup> Recent researches  
77 also showed that oleaginous bacteria, such as *Rhodococcus opacus* PD630, may have the  
78 potential capacity to use lignin as sole carbon resource for lipid production.<sup>17</sup> In addition,  
79 oleaginous yeast can also be used for converting biomass hydrolysates<sup>18</sup>. Even though the overall  
80 conversion rate of carbohydrates-to-lipid is much lower than that of ethanol, the oleaginous  
81 fungus-based platform has at least three major advantages. First, from a broader biodiesel  
82 industry perspective, lignocellulosic biomass provides a reliable feedstock for the significant  
83 amount of lipid needed for biodiesel refineries. Second and more importantly, oleaginous fungal  
84 species have been widely used for biotransformation of aromatic compounds, suggesting the  
85 possibility of using these species to utilize lignin along with carbohydrates to biofuel products.<sup>19,</sup>  
86 <sup>20</sup> For example, we identified a fast-growing oleaginous fungus *C. echinulata* FR3 with the  
87 capacity to accumulate more than 40% of dry cell weight in lipids when grown on glucose.  
88 Previous studies indicated that other *C. echinulata* strains could transform complex aromatic  
89 compounds.<sup>19</sup> However, despite these promising findings, the particular strain has not been used  
90 to convert lignocellulosic biomass, and neither has oleaginous fungus been evaluated for lignin  
91 degradation capacity during biomass conversion. Third and the most importantly, considering the  
92 potential to utilize lignin, this unique oleaginous strain may be used to convert biomass directly

93 without chemi-physical pretreatment. Even though different conversion platforms were  
94 developed to process different compositions of plant cell wall, few platforms can actually  
95 convert lignin together with carbohydrate into fungible fuels and products via biological  
96 processes. The study aims to offer an alternative approach where a simple biological system  
97 could convert all the composition of plant cell wall into biofuel product without additional  
98 pretreatment process.

99 Therefore, we will evaluate the possibility of such system with three aspects of studies. **First**,  
100 we evaluated whether the oleaginous fungus *C. echinulata* FR3 can convert lignin while  
101 processing carbohydrate. **Second**, we investigated if lignin modification of feedstock can be  
102 integrated with this oleaginous fungus strain to improve efficiency of biomass conversion  
103 without chemical pretreatment. **Third**, we further investigated the mechanisms for lignin  
104 utilization by oleaginous fungi using transcriptomics and chemical analysis. The discovery  
105 indicated that oleaginous fungus like FR3 can be exploited for complete biomass utilization in a  
106 consolidated platform without chemical pretreatment, or can be enhanced to convert lignin waste  
107 into lipid. These novel oleaginous fungus-based platforms could have profound impacts on  
108 energy and environmental sustainability when implemented.

109

## 110 **2. Material and Supplies**

### 111 2.1. Microorganism maintenance and spore inoculum preparation

112 *C echinulata* FR3 was isolated by Key Laboratory of Molecular Biophysics at Huazhong  
113 University of Science and Technology, and identified by China General Microbiological Culture  
114 Collection Center in Beijing. The strain was maintained at 4°C on potato dextrose agar (PDA)  
115 slant. To prepare the spore inoculum, the fungal mycelium was incubated on PDA in 250mL

116 Erlenmeyer flasks at 28°C for 5 days to form spores. The spores were then collected by washing  
117 the mycelium with 10mL sterile water and transferred to 100mL of potato dextrose broth (PDB)  
118 medium in 250mL Erlenmeyer flask with a final spore concentration of  $3 \times 10^7$  spores/L. The  
119 inoculation was cultivated at 28°C with a shaking speed of 150rpm for 36h.

## 120 2.2. Sorghum biomass

121 The signal- and double- mutant sorghum stocks were developed as previously described.<sup>21</sup>  
122 The wild-type and mutant lines of sorghum were grown in randomized block design at  
123 University of Nebraska Agricultural Research and Development fields near Mead, NE in 2010.  
124 The samples consisted of bulk biomass harvested from 4 plots. The grain heads were removed  
125 and sorghum lignocellulosic tissue (leaves and stalks) were dried at 50°C in air-blowing oven for  
126 3 days. The tissue was ground using a Wiley<sup>®</sup> mill (2-mm screen; Arthur H. Thomas Co.,  
127 Philadelphia, PA).

## 128 2.3. Dilute-acid pretreatment

129 The dilute-acid pretreatment of sorghum was carried out by mixing with diluted sulfuric acid  
130 to a final concentration of 1.5% (w/w) at a solid loading of 1:17 (w/v). The mixture was  
131 maintained at 121°C for 1h. After the reaction, the samples were neutralized to pH 7.0 with 2M  
132 sodium hydroxide.

## 133 2.4. Enzymatic hydrolysis and fungal conversion

134 For untreated sorghum stover enzymatic hydrolysis, samples were adjusted with distilled  
135 water to a solid loading of 1:17 (w/v) and autoclaved at 121°C for 20 min with liquid cycle.  
136 Different cellulase enzyme (Sigma, C2730) loading (3.0, 4.5 and 6.0 FPU/g sorghum) were used  
137 for hydrolysis at 28°C on a rotary shaker incubator at 150rpm for 48h. For the acid-pretreated  
138 wild-type sorghum, the cellulase was directly added to the neutralized sample with an enzyme

139 loading of 4.5 FPU/g sorghum biomass. The hydrolysis reactions were conducted as  
140 aforementioned. After hydrolysis, the pre-cultured *C. echinulata* FR3 were inoculated at a 5%  
141 (v/v) fungal biomass loading, and cultured on a rotary shaker incubator at 28°C and 150rpm.

#### 142 2.5. Sorghum biomass and mycelium biomass evaluation

143 The sorghum and mycelium biomass from the fermentation were harvested every 72-hour  
144 period (0, 3, 6 and 9 days) by centrifugation. The fungal mycelium pellets were separated from  
145 the sorghum biomass manually, and both the sorghum and fungal mycelium were washed with  
146 distilled water twice and dried at 60°C for three days to a constant weight. After drying, the  
147 weight of both sorghum and fungal mycelium was measured and recorded.

#### 148 2.6. Measurement of reducing sugar, cellulase and xylanase activity

149 The cultivation supernatant was collected by centrifugation to measure reducing sugar  
150 concentration, cellulase, and xylanase activities. Reducing sugar was measured with the DNS  
151 (3,5-dinitrosalicylic acid) reagent using the absorbance at 540 nm with a glucose standard  
152 curve.<sup>22</sup> The cellulase activity in the medium was assayed based on the ‘filter-paper-unit (FPU)’  
153 following the Laboratory Analytical Procedure (LAP 006) from the National Renewable Energy  
154 Laboratory (NREL). The xylanase activity was assayed using xylan as the substrate to measure  
155 the release of reducing sugar by DNS method by reaction of 30 min at 37°C and pH 4.8. One unit  
156 of xylanase activity was calculated as 1  $\mu$ mole of reducing sugar from xylan per min at the  
157 reaction condition.

#### 158 2.7. Lipid production evaluation

159 The extraction and composition analysis of total lipid were achieved by GC/MS (gas  
160 chromatograph/mass spectrometry) according the protocol described in our previous study.<sup>23</sup> The  
161 total lipid of the fungal mycelium was extracted in the form of fatty acid methyl ester (FAME)



162 with sulfuric acid–methanol method and collected in pre-weighted tubes. The tube with extracted  
163 FAME was further dried to a constant weight and then be weighted to derive the lipid yield.

164 The lipid composition was analyzed by GC/MS using an Agilent 7890 GC (Agilent  
165 Technologies, Santa Clara, CA) coupled with an Agilent 5975 mass spectrometer. An HP-5MSI  
166 column was used. The injection port was kept at 280 °C and the MS transfer line was set to  
167 100 °C. The GC oven temperature was programmed as follows: initial with 40 °C (0.5 min),  
168 increase to 110 °C at 5 °C/min, and then increase from 110 to 300 °C at 20 °C/min for a total run  
169 time of 24 min. The raw chromatography and mass spectra data were processed with software  
170 Enhanced ChemStation (Agilent Technologies, Santa Clara, CA), and the quantity of the specific  
171 lipid molecules was analyzed by the peak area.

## 172 2.8. Compositional analysis

173 Structural carbohydrates (cellulose and hemicellulose), lignin, and ash content of sorghum  
174 stovers were determined according to Laboratory Analytical Procedure from the National  
175 Renewable Energy Laboratory (NREL).<sup>24</sup> Carbohydrate concentrations were analyzed using  
176 high-performance liquid chromatography (HPLC 1260 Infinity; Agilent Technologies,  
177 CA). HPLC analyses were carried out with an Aminex HPX-87P Column (300 mm by 7.8 mm;  
178 Bio-Rad Laboratories, CA) with HPLC grade water as mobile phase and a flow rate of 0.6  
179 mL/min at 85°C using RI detector. The lignin, cellulose and hemicellulose degradation  
180 efficiencies were calculated as following:

181 Lignin (cellulose, hemicellulose) lost (%)

$$182 = \frac{100 - \text{lignin (cellulose,hemicellulose)content in converted sorghum} \times \text{final weight of sorghum after conversion}}{\text{lignin (cellulose,hemicellulose)content in raw sorghum} \times \text{inicial weight of raw sorghum}}$$

183

## 184 2.9. Solid state <sup>13</sup>C CP/MAS NMR analysis

185 The carbon-13 cross-polarization (CP) magic angle spinning (MAS) ( $^{13}\text{C}$  CP/MAS) Solid-  
186 state NMR was carried out to confirm the compositional and chemical changes of the structural  
187 components for sorghum biomass under different treatments. The control biomass tissues (250  
188 mg) and samples after conversion were individually packed in 5-mm pencil type rotor and the  
189 spectra were recorded under identical acquisition parameters. The solid state  $^{13}\text{C}$  CP/MAS  
190 analysis were carried out at 100 MHz on a Bruker Avance 400 spectrometer, (NMR center,  
191 Washington State University), equipped with a Chemagnetics double resonance probe. A contact  
192 time of 0.5 ms, proton field ca. 40 kHz during CP and data acquisition, relaxation delay of 4 s  
193 and spinning speed of 5 kHz were applied to obtain the  $^{13}\text{C}$  CP/MAS spectra. All the  
194 corresponding  $^{13}\text{C}$  CP/MAS spectra were derived from 17,500 scans, with the chemical shifts  
195 given in  $\delta$  ppm. The integrals for each resonance and/or chemical shift values arising from the  
196 cell wall components of fungal converted biomass were normalized with reference to their  
197 corresponding control spectra for semi-quantitative analysis.

#### 198 2.10. Transcriptomics analysis

199 The total RNA was extracted from *C. echinulata* FR3 grown on sorghum for 6 days with  
200 Qiagen RNeasy Plant Mini Kit. The transcriptomics sequencing of the fungal samples were  
201 performed using Illumina HiSeq 2500 by Institute of Plant Genomics and Biotechnology, Texas  
202 A&M University. The resulting reads were assembled with Trinity.<sup>25</sup> To further reduce the  
203 redundancy of the assembled transcripts, sequence clustering package CD-HIT were used to  
204 cluster similar sequence that meet similarity threshold  $>0.9$  into unigene clusters.<sup>26</sup> Unigenes  
205 were then functionally annotated based on UniProtKB (<http://www.uniprot.org/>) database by the  
206 package of ncbi-blast-2.2.28+ with the threshold of  $e < 10^{-6}$ . To quantify the expression level of  
207 unigenes, sequencing reads were mapped to the unigene sequences. Gene expression abundance

208 was calculated as normalized mapping read counts per million total mapping reads per kb of the  
209 gene length. The assembled unigenes were also aligned to CAZy database based on sequence  
210 similarity to carry out the lignocellulolytic degradation functional analysis through the  
211 Bioenergy Science Center web service ([http://mothra.ornl.gov/cgi-  
212 bin/cat/cat\\_v2.cgi?tab=ORTHOLOGS](http://mothra.ornl.gov/cgi-bin/cat/cat_v2.cgi?tab=ORTHOLOGS)) with E-value threads  $\leq 10^{-6}$  and Pfam domains bit score  
213 threshold  $\geq 100$ . The phylogenetic analysis was based on PhyML through Phylogeny.fr web  
214 server.<sup>27, 28</sup>

### 215 2.11. Determination of iron-reducing activity

216 Iron-reducing activity was determined based on formation of ferrozine-Fe<sup>2+</sup> complex.<sup>22</sup>  
217 2ml of cultivation supernatants collected by centrifugation were mixed with 0.5ml FeCl<sub>3</sub> (1.2mM)  
218 and 0.5ml ferrozine (15mM), and immediately measure the absorbance change at 562 nm with  
219 UV-Visible spectrometer for 3min. 1 unite (A/min) of iron-reducing activity was defined as the  
220 rate of absorbance increase at 562nm per minute.

## 221 3. Results and Discussion

### 222 3.1 *C. echinulata* FR3 (FR3) can degrade all cell wall components including cellulose, 223 hemicellulose, and lignin

224 Biomass composition analysis confirmed the reduced lignin content in the *bmr* lines (Table  
225 S1).<sup>13, 29</sup> *C. echinulata* FR3 fermentation led to the degradation of all cell wall structural  
226 components including lignin. Relatively lower cellulase loadings (3.0, 4.5 and 6.0 FPU/g  
227 sorghum) were used for saccharification (Figure S1), because oleaginous fungi can secrete  
228 cellulases for saccharification.<sup>16, 23</sup> Both the *bmr6* and the *bmr6/bmr12* double mutants allowed  
229 higher scarification efficiency than that of wild-type (Figure S1). The sorghum biomass  
230 hydrolyzed with 4.5 FPU/g enzyme load was then subjected to *C. echinulata* FR3 fermentation

231 to evaluate the degradation of different cell wall components. As shown in Figure 1A, weight  
232 loss was observed for cellulose, hemicellulose and lignin during the first six days of fermentation.  
233 The weight loss reached a plateau at day 6 to day 9 for most of the samples. In general, a higher  
234 percentage of weight loss was achieved for all mutants as compared to wild-type (Figure 1). In  
235 particular, more significant lignin weight loss was found for both *bmr12* and *bmr6/bmr12* double  
236 mutants. For example, the lignin weight loss for double mutant and wide-type was 46% and 31%,  
237 respectively (Figure 1B). More significant cellulose weight loss was observed for both *bmr6* and  
238 the *bmr6/bmr12* double mutants (Figure 1C). The fermentation of *bmr6* mutant led to the most  
239 significant hemicellulose weight loss (Figure 1D). The significant degradation of cell wall lignin  
240 in *C. echinulata* FR3 is noteworthy as the phenomena is normally common to Basidiomycetes,  
241 but not to other genera of fungi. As an oleaginous fungus, the capacity to degrade lignin over 30%  
242 offers *C. echinulata* FR3 new opportunities of utilization of multiple cell wall components for  
243 useful products and the bioconversion without chemical pretreatment.

### 244 **3.2. Lignin modification promoted biomass conversion by *C. echinulata* FR3**

245 The biomass weight loss correlated well with the growth of *C. echinulata* FR3. In general,  
246 *C. echinulata* FR3 grew faster and accumulated more fungal biomass on *bmr* mutants, which  
247 was consistent with the greater sorghum biomass weight loss in *bmr* mutants (Figure 2A). The  
248 fungal cell growth reached plateau phase at Day 6, when the sorghum biomass weight loss also  
249 turned to plateau phase. Among the three mutant lines of sorghum, FR3 grown on *bmr6/bmr12*  
250 double mutant and *bmr12* mutant accumulated higher cell biomass as compared to that of *bmr6*  
251 and wild-type (Figure 2A).

252 The weight loss and fungal growth also correlated with lipid yield. The lipid yield for all  
253 fermentation experiments increased during the first six days and decreased on Day 9 (Figure 2B).

254 The result could be explained by the fact that both fungal growth and sorghum biomass weight  
255 loss reached plateau at Day 6. The fungus might start catabolizing lipids after Day 6, because the  
256 reduced sugar also reached plateau phase at Day 6 (Figure S2). Day 6 thus represented the  
257 optimal time to harvest and compare lipid yields among different lines. Among the three *bmr*  
258 lines, both *bmr6* and *bmr6/bmr12* double mutants yielded more lipid during fermentation. The  
259 fermentation of *bmr6/bmr12* led to the most significant increase in lipid production.

260 In order to further elucidate the mechanisms for biomass degradation, we analyzed reduced  
261 sugar and enzyme activities in the fermentation system. As aforementioned, the level of reduced  
262 sugar dropped rapidly during the first six days of fermentation and reached a plateau at Day 6 to  
263 Day 9 (Figure S2). The enzyme activity reached peak level at Day 3 (Figure 2C and D).  
264 Considering that the exogenous cellulase was added two days before Day 0, the result clearly  
265 indicated that endogenous cellulase played an important role in the biomass degradation and  
266 fungal cell growth. The results in enzyme and reducing sugar analysis were consistent with the  
267 fungal growth and lipid yield. Besides the cellulose and hemicellulose, detailed analysis of lignin  
268 content was carried out using NMR spectroscopy to further confirm lignin degradation.

### 269 3.3.NMR analysis confirmed the degradation of lignin along with carbohydrates

270 In order to further confirm that *C. enchinulata* FR3 could convert lignin along with the  
271 carbohydrates, the solid-state NMR was carried out to analyze sorghum biomass using the  
272 conventional CP/MAS (cross-polarization-magic angle spinning) method.<sup>30</sup> The analysis was  
273 focused on the structural changes of the wild-type and *bmr6/bmr12* double mutant sorghum after  
274 6-days fungal conversion as compared to the reference samples without fermentation. The  
275 normalized <sup>13</sup>C CP/MAS NMR spectrums were depicted in Figure S3 and Figure S4 and the  
276 most predominant assignments for each resonance peak were listed in Table S2.<sup>31, 32</sup> The

277 acquired spectra mainly contained chemical resonance values analogous to carbohydrate region  
278 (60-100 ppm) and aromatic region (100-162 ppm). In addition, the chemical shift resonances of  
279 carbonyl and carboxyl group (160-200 ppm), methoxyl group (52-55 ppm) and carbon in  
280 etherified and/or non-etherified region (132-152 ppm) were also observed. The comparison of  
281  $^{13}\text{C}$  CP/MAS NMR spectra among different samples revealed several features.

282 First, comparison of aromatic carboxyl resonances (165-175 ppm) indicated the significant  
283 differences in the lignin derived aromatic region (Figure S4A). The results suggested that FR3  
284 conversion of sorghum biomass resulted in lignin utilization, confirming the lignin weight loss  
285 data. Second, the  $^{13}\text{C}$  CP/MAS NMR analysis showed reduced intensity in the aliphatic  
286 carbonyl/carboxyl group resonances (175- 185 ppm) for both wild-type and *bmr6/bmr12* mutant  
287 after conversion by *C. enchinulata* FR3. The result strongly indicated the removal of  
288 hemicelluloses and side chain alterations in lignin macromolecular assembly,<sup>33</sup> which could  
289 result from cell wall deconstruction by *C. enchinulata* FR3 during the 6-days conversion process.  
290 Third, in contrast to the aforementioned decreases, a slight increase in the intensity at chemical  
291 shift values of 60-90 ppm (carbohydrate region) was observed in the biomass samples after  
292 fungal conversion. Such increase was due to the relatively more rapid reduction in the content of  
293 aromatic lignin and aliphatic carbon. The result suggested that the lignin degradation was more  
294 rapid than cellulose degradation during the six days of conversion by *C. enchinulata* FR3. The  
295 result was consistent with composition analysis. The quantification of resonances with reference  
296 to the control  $^{13}\text{C}$  CP/MAS NMR spectra was also carried out under normalized condition to  
297 determine the contents (in %) of cell wall components in the corresponding samples (Table 1).  
298 The results further confirmed the degradation of all cell wall components including cellulose,  
299 hemicellulose and lignin by *C. enchinulata* FR3 conversion. In addition, Table 1 further

300 confirmed more rapid degradation of lignin, as the aromatic contents in wild-type and  
301 *bmr6/bmr12* mutant after conversion were reduce to 12.1% and 13.0% respectively, as compared  
302 to 16.8% and 18.6% in the untreated controls. Overall, the biomass composition analysis and <sup>13</sup>C  
303 CP/MAS NMR analysis were highly consistent to demonstrate that *C. echinulata* FR3 could  
304 degrade all the plant cell wall composition including lignin, cellulose, and hemicellulose.

### 305 **3.4. Similar lipid yield can be achieved for fermentation of *bmr* mutant and acid-pretreated** 306 **wild-type biomass**

307 The consumption of lignin by oleaginous fungus suggested that *C. echinulata* FR3  
308 conversion of sorghum biomass might alter lignin content and structure, in a process similar to  
309 biological pretreatment by white rot fungus. We therefore hypothesized that biomass conversion  
310 might be carried out without chemical pretreatment, if biomass has a relatively low recalcitrance.  
311 We further compared the fungal growth and lipid yield of *C. echinulata* FR3 grown on acid-  
312 pretreated wild-type and non-pretreated *bmr6/bmr12* double mutant sorghum stover after 6 days  
313 (Figure 3A). Even though acid-pretreated wild-type sorghum led to a much higher weight loss  
314 (65.5%) than non-pretreated *bmr6/bmr12* sorghum (Figure 3B), no significant difference on the  
315 cell growth and lipid production were found between the two types samples (Figure 3A).The  
316 greater weight lose might be caused by the degradation of hemicellulose by sulfate acid during  
317 the pretreatment (Figure 3C). The GC/MS analysis also revealed that the lipid profile of *C.*  
318 *echinulata* FR3 has no significant difference between the two conditions (Figure S5). It is well  
319 established that various inhibitors and toxins could be generated during the dilute acid  
320 pretreatment to inhibit microbial growth.<sup>34, 35</sup> The inhibitors and toxins might also inhibit the cell  
321 growth and cause low lipid yield during biomass conversion by oleaginous fungus *C. echinulata*  
322 FR3.

### 323 3.5. Transcriptomics analysis revealed lignin and biomass degradation mechanism in FR3

324 Even though some filamentous fungi could degrade the lignocellulosic biomass, few studies  
325 indicated that any non-basidiomycetous filamentous fungi could degrade lignin. In particular, the  
326 lignin degradation capacity in oleaginous fungi might be exploited for broad applications  
327 including complete biomass utilization, consolidated biomass processing, and lignin conversion  
328 to lipid. The development of these new platforms will depend on in-depth understanding of  
329 biomass and lignin degradation mechanisms in *C. echinulata* FR3. Transcriptomics analysis of  
330 FR3 grown on the wild-type and *bmr6/bmr12* mutant was carried out to further explore the  
331 mechanisms for biomass, in particular, lignin degradation.

332 The result revealed that *C. echinulata* FR3 synergized extracellular lignocellulolytic enzymes  
333 and radical systems for biomass degradation. The transcriptomics analysis revealed three features.  
334 First, FR3 had cellulase enzymes, but not in a balanced combination to achieve maximized  
335 cellulose and hemicellulose degradation (Figure 4A). The analysis based on CAZy database  
336 revealed that cellulose and hemicellulose degradation enzymes were expressed, which was  
337 consistent with the cellulase and xylanase activity detected. Among the 17312 predicated gene  
338 models, 502 belonged to different CAZy families (bit score  $\geq 100$ ), including 131 glycoside  
339 hydrolases (GH) and 55 carbohydrate esterases (CE) (Figure S6). Despite the prevalence of GH  
340 enzymes, only 2 endoglucanase, 2 beta-1,4-glucosidase and 1 exoglucanase were identified.  
341 Among these cellulolytic enzymes, only CeFR966 encoding endoglucanase (GH9) was  
342 expressed at a high level (Figure 4A). The result indicated that *C. echinulata* FR3 had  
343 carbohydrate degradation capacity, yet the capacity is limited as compared to most of other  
344 cellulose degradation fungi.



345 Second, an alternative extracellular lignolytic enzyme system was identified in *C. echinulata*  
346 FR3 (Figure 4B). The enzyme system is slightly different from the classic lignolytic enzyme  
347 system based on peroxidases and laccases in white rot fungi.<sup>36</sup> Several gene models were  
348 annotated to be multiple copper oxidases, and one of them, CeFR1943, encoded a laccase-like  
349 multiple copper oxidases (LMCO) with a secretion signal peptide sequence. Phylogenetic  
350 analysis of this LMCO with classic laccases from fungi (ascomycetes and basidiomycetes) and  
351 plants revealed that the enzyme was related to basidiomycete fungal laccases known for strong  
352 lignin degradation capacity. The results indicated that the LMCO might involve in lignin  
353 depolymerization in *C. echinulata* FR3. Meanwhile, another gene CeFR715 encoded aromatic  
354 peroxygenase (APO) with predicted secretive signal peptides. Extracellular APOs were a novel  
355 group of heme-thiolate enzymes characterized for lignin degradation by catalyzing H<sub>2</sub>O<sub>2</sub>-  
356 dependent oxidative cleavage of diverse ethers in aromatic substrates.<sup>37-39</sup> The transcriptomics  
357 analysis thus suggested that LMCO and APO might be the main extracellular lignolytic  
358 enzymes for *C. echinulata* FR3.

359 Third, a strong radical generation system was identified for *C. echinulata* FR3 and the  
360 radicals can synergize either with the aforementioned oxidative enzymes or with the iron-  
361 quinone system for Fenton reaction. Many enzymes contributing to extracellular H<sub>2</sub>O<sub>2</sub> generation  
362 were discovered from the transcriptomics analysis (Figure 4B). Copper radical oxidase (CRO)  
363 and GMC oxidoreductase were two major groups involved with extracellular H<sub>2</sub>O<sub>2</sub> generation  
364 for Fenton system in most studied fungi system.<sup>40-42</sup> Unlike the basidiomycetes expressing  
365 several CROs, only one CRO, CeFR251, was identified in *C. echinulata* FR3 encoding galactose  
366 oxidase with predicted secretive signal peptides. Moreover, this gene was expressed in a very  
367 high level as compared to many other genes (Figure 4B). At the meanwhile, several GMC

368 oxidoreductase-type genes were identified encoding long-chain-alcohol oxidase. These resulted  
369 indicated that *C. echinulata* FR3 thus had a system to generate extracellular H<sub>2</sub>O<sub>2</sub>.

370 Fourth, the identification of iron reduction related proteins further suggested that the radical  
371 generation synergized with Fenton reaction (Figure 4B). Besides the extracellular enzymes,  
372 wood degradation by basidiomycetes often involved extracellular low molecular weight oxidants,  
373 particularly Fenton reaction generated hydroxyl radicals.<sup>40, 43-45</sup> The transcriptomics analysis  
374 suggested that *C. echinulata* FR3 also had the similar Fenton reaction-based radical system for  
375 lignin depolymerization. Several gene models (CeFR296, CeFR2458, CeFR 2745 and CeFR8451)  
376 were identified as putative quinone reductases (QRD) and were expressed in a relative high level.  
377 Redox cycling of secreted quinones was considered as a driving force for Fenton reaction in  
378 wood-degrading fungus.<sup>46, 47</sup> The expression of these putative QRD in coordination with quinate  
379 permeases (CeFR7596 and CeFR10458) for the biosynthesis and transport of quinones might  
380 enable an efficient extracellular Fenton system. In addition to the quinone-based iron reduction  
381 system, transmembrane ferric reductase (CeFR10940) was also found expressed with possible  
382 Fe<sup>3+</sup> reduction function.

383 Overall, the transcriptomics analysis revealed a unique lignocellulose degradation system in  
384 *C. echinulata* FR3 by synergizing extracellular lignocellulolytic enzymes and hydroxyl radicals  
385 (Figure 5). Such system has enabled *C. echinulata* FR3 to become one of few known strains  
386 outside of basidiomycetes with an appreciable lignin degradation capacity. During biomass  
387 degradation, *C. echinulata* FR3 could express extracellular H<sub>2</sub>O<sub>2</sub>-generation related  
388 oxidoreductases (mainly galactose oxidase) and ferric reduction related proteins (QRD and ferric  
389 reductase) to mediate the Fenton reaction ( $\text{Fe}^{2+} + \text{H}_2\text{O}_2 \rightarrow \text{Fe}^{3+} + \cdot\text{OH} + \text{OH}^-$ ). The generated  
390 hydroxyl radicals from Fenton-based system could both depolymerize polysaccharides and lignin

391 to make the lignocellulose more accessible for lignocellulolytic enzymes.<sup>40, 44, 48</sup> For lignin  
392 depolymerization, extracellular APO and LMCO could synergize with hydroxyl radical to carry  
393 out efficient lignin depolymerization in a way different from basidiomycetes. For cellulose and  
394 hemicellulose degradation, the enzymatic cellulose degradation pattern of *C. echinulata* FR3 was  
395 very similar to many of brown rot fungi, in which endoglucanases were highly expressed whilst  
396 cellobiohydrolases were poorly expressed or even absent during the cellulose degradation.<sup>49</sup>  
397 After the lignin depolymerization process, the released small molecular aromatic compounds  
398 could be transported into the cell for complete aromatic compound catabolism. Pathway analysis  
399 revealed two central aromatic catabolism pathways involving the ring-cleaving of homogentisate  
400 and 3-hydroxyanthranilate (Figure 4C).<sup>50</sup> Numerous cytochrome P450s (~50 genes) were also  
401 discovered in *C. echinulata* FR3, indicating that cytochrome P450s may involve in  
402 degradation/conversion of the lignin derived metabolites into central aromatic intermediates for  
403 complete degradation as previously reported.<sup>51, 52</sup>

### 404 **3.6. Enzyme assay further confirms that Fenton reaction is one of the mechanisms for lignin** 405 **degradation in *C. echinulata* FR3**

406 In order to further verify the role of radicals and Fenton reaction in lignin degradation, iron-  
407 reducing activity was measured as an indicator for hydroxyl radical levels. The hydroxyl radical  
408 level is often impacted by iron reducing capacity, which is important in Fenton reaction. As  
409 shown in Figure 6, the iron-reducing activity significantly increased in the *C. echinulata* FR3  
410 grown on biomass as compared to that on PDB medium. No significant difference was observed  
411 for iron reducing activity of fungus grown on wild-type and *bmr6/bmr12* mutant sorghum. The  
412 significant induction of iron-reducing activity throughout the biomass fermentation process

413 indicated that the induced Fenton reaction system might play an important role in lignin and  
414 biomass degradation, confirming the transcriptomics data.

### 415 **3.7. Perspectives on oleaginous fungus with strong lignin degradation capacity**

416 Overall, the biomass composition, chemical, and genomic data all suggested that oleaginous  
417 fungus *C. echinulata* FR3 has a unique capacity to efficiently utilize lignin. The discovery of an  
418 oleaginous fungus with strong lignin degradation capacity could be significant from several  
419 perspectives. First, even though lignin degradation by fungi has been studied extensively in  
420 basidiomycetes, few studies indicated that the capacity exists in filamentous fungi beyond  
421 basidiomycetes. From a scientific perspective, the genomic and molecular mechanisms for lignin  
422 degradation in *C. echinulata* FR3 and its relatedness to the mechanisms in basidiomycetes  
423 indicated that additional species evolved lignin degradation capacity in a convergent way using  
424 different mechanisms. From the application perspective, the oleaginous fungus with lignin  
425 degradation capacity will bridge an important limitation as white rot fungus has not been known,  
426 to date, to produce a fungible product from biomass. Second, the lignin degradation capacity in  
427 oleaginous fungi could enable a highly consolidated platform for biomass conversion, where  
428 chemi-physical pretreatment might not be necessary. The combination of lignin modification  
429 with fungal fermentation has already reached similar performance in terms of lipid yield (Figure  
430 3). Such capacity can be further enhanced by genetic modification or condition optimization to  
431 achieve a more consolidated process. However, it should be pointed out that the limitation of  
432 FR3 fermentation is the relatively weak cellulose and hemicellulose degradation capacity. Third,  
433 the strong lignin degradation capacity also indicated it is possible for FR3 to be utilized for the  
434 conversion of lignin. A fungus-based lipid production platform is often robust and more  
435 amenable to small to mid-size operations. The lignin utilization capacity and potential for

436 consolidated processing will enable these strengths. The utilization of lignin modification  
437 mutants may further enhance the advantages. Further engineering of FR3 and optimization of  
438 fermentation conditions are necessary to enable such platforms.

#### 439 **4. Conclusions**

440 In summary, we have revealed that the oleaginous fungi *C. echinulata* FR3 can accumulate  
441 high levels of lipid by degrading all the component of plant cell wall including lignin, cellulose,  
442 and hemicellulose. The biomass composition analysis and NMR-based structure analysis  
443 indicated *C. echinulata* FR3 degraded lignin with higher efficiency than cellulose/hemicellulose.  
444 Further transcriptomics studies and biochemical studies revealed that lignocellulose degradation  
445 in *C. echinulata* FR3 involved both extracellular lignocelulolytic enzymes and Fenton-system-  
446 mediated hydroxyl radicals. In addition, lignin modification in plant feedstock could improve the  
447 lignocellulose-to-lipid conversion efficiency by *C. echinulata* FR3. In an extreme case, the  
448 lignin-modified sorghum feedstock could be used for *C. echinulata* FR3 fermentation to yield  
449 similar amount of lipid as compared to pretreated wild-type plants. The study thus suggested that  
450 combining feedstock lignin modification with oleaginous fungal fermentation might deliver a  
451 cost-efficient bioconversion platform without chemical pretreatment. Considering the unique and  
452 strong lignin degradation capacity, the oleaginous fungus *C. echinulata* FR3 could serve as the  
453 base strain for further genetic engineering to achieve a sustainable and economic lignocellulose-  
454 to-biodiesel platform.

#### 455 **5. Acknowledgement**

456 The work in China was supported by a grant from the National High-tech Research and  
457 Development Program of China (Grant No. 2011AA100904). The work in United States was  
458 supported by the U.S. DOE (Department of Energy) EERE (Energy Efficiency and Renewable

459 Energy) BETO (Bioenergy Technology Office) Grant (No. DE-EE0006112) to JSY and BY. The  
460 research is also supported by Texas A&M Agrilife Research's biofuel initiative to JSY.  
461

## 462 Reference

- 463 1. L. R. Lynd, M. S. Laser, D. Bransby, B. E. Dale, B. Davison, R. Hamilton, M. Himmel,  
464 M. Keller, J. D. McMillan, J. Sheehan and C. E. Wyman, *Nat. Biotechnol.*, 2008, **26**,  
465 169-172.
- 466 2. B. Yang and C. E. Wyman, *Biotechnol. Bioeng.*, 2004, **86**, 88-95.
- 467 3. S.-Y. Ding, Y.-S. Liu, Y. Zeng, M. E. Himmel, J. O. Baker and E. A. Bayer, *Science*,  
468 2012, **338**, 1055-1060.
- 469 4. F. Chen and R. A. Dixon, *Nat. Biotechnol.*, 2007, **25**, 759-761.
- 470 5. J. S. Yuan, K. H. Tiller, H. Al-Ahmad, N. R. Stewart and C. N. Stewart, Jr., *Trends Plant*  
471 *Sci.*, 2008, **13**, 421-429.
- 472 6. R. Franke, C. M. McMichael, K. Meyer, A. M. Shirley, J. C. Cusumano and C. Chapple,  
473 *Plant J.*, 2000, **22**, 223-234.
- 474 7. F. Chen, M. S. Srinivasa Reddy, S. Temple, L. Jackson, G. Shadle and R. A. Dixon,  
475 *Plant J.*, 2006, **48**, 113-124.
- 476 8. C. Fu, J. R. Mielenz, X. Xiao, Y. Ge, C. Y. Hamilton, M. Rodriguez, Jr., F. Chen, M.  
477 Foston, A. Ragauskas, J. Bouton, R. A. Dixon and Z. Y. Wang, *Proc. Natl. Acad. Sci. U*  
478 *SA*, 2011, **108**, 3803-3808.
- 479 9. A. Saballos, W. Vermerris, L. Rivera and G. Ejeta, *BioEnergy Research*, 2008, **1**, 193-  
480 204.
- 481 10. X. Li, J. K. Weng and C. Chapple, *Plant J.*, 2008, **54**, 569-581.
- 482 11. K. S. Porter, J. D. Axtell, V. L. Lechtenberg and V. F. Colenbrander, *Crop Sci.*, 1978, **18**,  
483 205-208.
- 484 12. Z. Xin, M. L. Wang, N. A. Barkley, G. Burow, C. Franks, G. Pederson and J. Burke,  
485 *BMC Plant Biol.*, 2008, **8**, 103.
- 486 13. N. A. Palmer, S. E. Sattler, A. J. Saathoff, D. Funnell, J. F. Pedersen and G. Sarath,  
487 *Planta*, 2008, **229**, 115-127.
- 488 14. B. S. Dien, G. Sarath, J. F. Pedersen, S. E. Sattler, H. Chen, D. L. Funnell-Harris, N. N.  
489 Nichols and M. A. Cotta, *BioEnergy Research*, 2009, **2**, 153-164.
- 490 15. J. Zeng, Y. Zheng, X. Yu, L. Yu, D. Gao and S. Chen, *Bioresour. Technol.*, 2013, **128**,  
491 385-391.
- 492 16. H. Wei, W. Wang, J. M. Yarbrough, J. O. Baker, L. Laurens, S. Van Wychen, X. Chen, L.  
493 E. Taylor, II, Q. Xu, M. E. Himmel and M. Zhang, *PLoS One*, 2013, **8**, e71068.
- 494 17. M. Kosa and A. J. Ragauskas, *Green Chemistry*, 2013, **15**, 2070-2074.
- 495 18. C. Hu, X. Zhao, J. Zhao, S. Wu and Z. K. Zhao, *Bioresour. Technol.*, 2009, **100**, 4843-  
496 4847.
- 497 19. T. J. Cutright, *Int. Biodeterior. Biodegrad.*, 1995, **35**, 397-408.
- 498 20. D. Münchnerová and J. Augustin, *Bioresour. Technol.*, 1994, **48**, 97-106.
- 499 21. J. F. Pedersen, J. J. Toy, D. L. Funnell, S. E. Sattler, A. L. Oliver and R. A. Grant, *J.*  
500 *Plant Reg.*, 2008, **2**, 258-262.
- 501 22. W. Du, H. Yu, L. Song, J. Zhang, C. Weng, F. Ma and X. Zhang, *Biotechnol. Biofuels*,  
502 2011, **4**, 1754-6834.
- 503 23. S. Xie, S. Sun, S. Y. Dai and J. S. Yuan, *Algal Research*, 2013, **2**, 28-33.
- 504 24. A. Sluiter, B. Hames, R. Ruiz, C. Scarlata, J. Sluiter, D. Templeton and D. Crocker,  
505 *Laboratory analytical procedure*, 2008.

- 506 25. M. G. Grabherr, B. J. Haas, M. Yassour, J. Z. Levin, D. A. Thompson, I. Amit, X.  
507 Adiconis, L. Fan, R. Raychowdhury, Q. Zeng, Z. Chen, E. Mauceli, N. Hacohen, A.  
508 Gnirke, N. Rhind, F. di Palma, B. W. Birren, C. Nusbaum, K. Lindblad-Toh, N.  
509 Friedman and A. Regev, *Nat. Biotechnol.*, 2011, **29**, 644-652.
- 510 26. W. Li and A. Godzik, *Bioinformatics*, 2006, **22**, 1658-1659.
- 511 27. A. Dereeper, V. Guignon, G. Blanc, S. Audic, S. Buffet, F. Chevenet, J. F. Dufayard, S.  
512 Guindon, V. Lefort, M. Lescot, J. M. Claverie and O. Gascuel, *Nucleic. Acids. Res.*, 2008,  
513 **36**, 19.
- 514 28. S. Guindon, J. F. Dufayard, V. Lefort, M. Anisimova, W. Hordijk and O. Gascuel, *Syst.*  
515 *Biol.*, 2010, **59**, 307-321.
- 516 29. B. Dien, G. Sarath, J. Pedersen, S. Sattler, H. Chen, D. Funnell-Harris, N. Nichols and M.  
517 Cotta, *BioEnergy Research*, 2009, **2**, 153-164.
- 518 30. G. J. Leary, K. R. Morgan, R. H. Newman, B. Samuelsson and U. Westermark, in *hfgs*,  
519 1986, vol. 40, p. 221.
- 520 31. X. F. Sun, R. Sun, P. Fowler and M. S. Baird, *J. Agric. Food Chem.*, 2005, **53**, 860-870.
- 521 32. G. Gilardi, L. Abis and A. E. G. Cass, *Enzyme Microb. Technol.*, 1995, **17**, 268-275.
- 522 33. D. Singh, J. Zeng, D. D. Laskar, L. Deobald, W. C. Hiscox and S. Chen, *Biomass*  
523 *Bioenergy*, 2011, **35**, 1030-1040.
- 524 34. J. Zhang, Z. Zhu, X. Wang, N. Wang, W. Wang and J. Bao, *Biotechnol. Biofuels*, 2010, **3**,  
525 1754-6834.
- 526 35. S. I. Mussatto and I. C. Roberto, *Bioresour. Technol.*, 2004, **93**, 1-10.
- 527 36. D. Floudas, M. Binder, R. Riley, K. Barry, R. A. Blanchette, B. Henrissat, A. T. Martínez,  
528 R. Otilar, J. W. Spatafora, J. S. Yadav, A. Aerts, I. Benoit, A. Boyd, A. Carlson, A.  
529 Copeland, P. M. Coutinho, R. P. de Vries, P. Ferreira, K. Findley, B. Foster, J. Gaskell, D.  
530 Glotzer, P. Górecki, J. Heitman, C. Hesse, C. Hori, K. Igarashi, J. A. Jurgens, N. Kallen,  
531 P. Kersten, A. Kohler, U. Kües, T. K. A. Kumar, A. Kuo, K. LaButti, L. F. Larrondo, E.  
532 Lindquist, A. Ling, V. Lombard, S. Lucas, T. Lundell, R. Martin, D. J. McLaughlin, I.  
533 Morgenstern, E. Morin, C. Murat, L. G. Nagy, M. Nolan, R. A. Ohm, A. Patyshakuliyeva,  
534 A. Rokas, F. J. Ruiz-Dueñas, G. Sabat, A. Salamov, M. Samejima, J. Schmutz, J. C. Slot,  
535 F. St. John, J. Stenlid, H. Sun, S. Sun, K. Syed, A. Tsang, A. Wiebenga, D. Young, A.  
536 Pisabarro, D. C. Eastwood, F. Martin, D. Cullen, I. V. Grigoriev and D. S. Hibbett,  
537 *Science*, 2012, **336**, 1715-1719.
- 538 37. C. Liers, T. Arnstadt, R. Ullrich and M. Hofrichter, *FEMS Microbiol. Ecol.*, 2011, **78**, 91-  
539 102.
- 540 38. M. J. Pecyna, R. Ullrich, B. Bittner, A. Clemens, K. Scheibner, R. Schubert and M.  
541 Hofrichter, *Appl. Microbiol. Biotechnol.*, 2009, **84**, 885-897.
- 542 39. M. Kinne, M. Poraj-Kobielska, S. A. Ralph, R. Ullrich, M. Hofrichter and K. E. Hammel,  
543 *J. Biol. Chem*, 2009, **284**, 29343-29349.
- 544 40. P. Kersten and D. Cullen, *Fungal Genet. Biol.*, 2007, **44**, 77-87.
- 545 41. A. Vanden Wymelenberg, G. Sabat, M. Mozuch, P. J. Kersten, D. Cullen and R. A.  
546 Blanchette, *Appl. Environ. Microbiol.*, 2006, **72**, 4871-4877.
- 547 42. C. O. Rohr, L. N. Levin, A. N. Mentaberry and S. A. Wirth, *PLoS One*, 2013, **8**, e81033.
- 548 43. A. Vanden Wymelenberg, J. Gaskell, M. Mozuch, G. Sabat, J. Ralph, O. Skyba, S. D.  
549 Mansfield, R. A. Blanchette, D. Martinez, I. Grigoriev, P. J. Kersten and D. Cullen, *Appl.*  
550 *Environ. Microbiol.*, 2010, **76**, 3599-3610.



- 551 44. D. Martinez, J. Challacombe, I. Morgenstern, D. Hibbett, M. Schmoll, C. P. Kubicek, P.  
552 Ferreira, F. J. Ruiz-Duenas, A. T. Martinez, P. Kersten, K. E. Hammel, A. Vanden  
553 Wymelenberg, J. Gaskell, E. Lindquist, G. Sabat, S. S. Bondurant, L. F. Larrondo, P.  
554 Canessa, R. Vicuna, J. Yadav, H. Doddapaneni, V. Subramanian, A. G. Pisabarro, J. L.  
555 Lavin, J. A. Oguiza, E. Master, B. Henrissat, P. M. Coutinho, P. Harris, J. K. Magnuson,  
556 S. E. Baker, K. Bruno, W. Kenealy, P. J. Hoegger, U. Kues, P. Ramaiya, S. Lucas, A.  
557 Salamov, H. Shapiro, H. Tu, C. L. Chee, M. Misra, G. Xie, S. Teter, D. Yaver, T. James,  
558 M. Mokrejs, M. Pospisek, I. V. Grigoriev, T. Brettin, D. Rokhsar, R. Berka and D. Cullen,  
559 *Proc. Natl. Acad. Sci. U S A*, 2009, **106**, 1954-1959.
- 560 45. C. Hori, J. Gaskell, K. Igarashi, M. Samejima, D. S. Hibbett, B. Henrissat and D. Cullen,  
561 *Mycologia*, 2013.
- 562 46. F. Guillen, C. Munoz, V. Gomez-Toribio, A. T. Martinez and M. Jesus Martinez, *Appl.*  
563 *Environ. Microbiol.*, 2000, **66**, 170-175.
- 564 47. J. Jensen, Kenneth A., Z. C. Ryan, A. Vanden Wymelenberg, D. Cullen and K. E.  
565 Hammel, *Appl. Environ. Microbiol.*, 2002, **68**, 2699-2703.
- 566 48. S. Xie, R. Syrenne, S. Sun and J. S. Yuan, *Curr. Opin. Biotechnol.*, 2014, **27**, 195-203.
- 567 49. D. C. Eastwood, D. Floudas, M. Binder, A. Majcherczyk, P. Schneider, A. Aerts, F. O.  
568 Asiegbu, S. E. Baker, K. Barry, M. Bendiksby, M. Blumentritt, P. M. Coutinho, D.  
569 Cullen, R. P. de Vries, A. Gathman, B. Goodell, B. Henrissat, K. Ihrmark, H. Kausrud,  
570 A. Kohler, K. LaButti, A. Lapidus, J. L. Lavin, Y.-H. Lee, E. Lindquist, W. Lilly, S.  
571 Lucas, E. Morin, C. Murat, J. A. Oguiza, J. Park, A. G. Pisabarro, R. Riley, A. Rosling, A.  
572 Salamov, O. Schmidt, J. Schmutz, I. Skrede, J. Stenlid, A. Wiebenga, X. Xie, U. Kues, D.  
573 S. Hibbett, D. Hoffmeister, N. Högberg, F. Martin, I. V. Grigoriev and S. C. Watkinson,  
574 *Science*, 2011, **333**, 762-765.
- 575 50. G. Fuchs, M. Boll and J. Heider, *Nat. Rev. Microbiol.*, 2011, **9**, 803-816.
- 576 51. D. Martinez, L. F. Larrondo, N. Putnam, M. D. Gelpke, K. Huang, J. Chapman, K. G.  
577 Helfenbein, P. Ramaiya, J. C. Detter, F. Larimer, P. M. Coutinho, B. Henrissat, R. Berka,  
578 D. Cullen and D. Rokhsar, *Nat. Biotechnol.*, 2004, **22**, 695-700.
- 579 52. H. Doddapaneni, V. Subramanian, B. Fu and D. Cullen, *Fungal Genet. Biol.*, 2013, **55**,  
580 22-31.

581

582

583 **Figure Legend:**

584 **Table 1.** Semi-quantitative analysis of cell wall components by  $^{13}\text{C}$  CPMAS NMR analysis. WT-  
585 raw: wild-type sorghum without fungal conversion; WT-6 days: wild-type sorghum after 6-days  
586 fungal conversion; b6b12-raw: *bmr6/bmr12* double mutant sorghum without fungal conversion;  
587 b6b12-6 days: *bmr6/bmr12* double mutant sorghum after 6-days fungal conversion.

588 **Figure 1.** Percentage of weight loss for total sorghum straw (A), lignin (B), cellulose (C) and  
589 hemicellulose (D) during the conversion of wild type (solid square), *bmr6* mutant (solid triangle),  
590 *bmr12* mutant (open square) and *bmr6/bmr12* double mutant (open triangle) sorghum biomass by  
591 *C. echinulata* FR3. The percentages of weight loss as compared to the original composition in  
592 raw sorghum biomass were recorded to represent the composition degradation efficiencies.

593 **Figure 2.** Mycelium growth (A) and lipid accumulation (B) of *C. echinulata* FR3 grown in  
594 sorghum biomass. FPU activity (C) and xylanase activity (D) of the cultivation supernatant  
595 variations during the conversion of wild type (solid square), *bmr6* mutant (solid triangle), *bmr12*  
596 mutant (open square) and *bmr6/bmr12* double mutant (open triangle) sorghum biomass by *C.*  
597 *echinulata* FR3. All assays were carried out in triplicates.

598 **Figure 3.** (A) Comparison of mycelium growth and lipid accumulation of *C. echinulata* FR3  
599 grown on acid-pretreated wild type (WT) sorghum straw and non-pretreated *bmr6/bmr12* double  
600 mutant (b6b12) sorghum straw for 6 days. (B) Comparison of total sorghum weight and lignin  
601 lost during the conversion of acid-pretreated wild-type and non-pretreated double mutant  
602 sorghum straw by *C. echinulata* FR3 after 6 days. (C) Comparison of cellulose and  
603 hemicellulose degradation during the conversion of acid-pretreated wild-type and non-pretreated  
604 double mutant sorghum straws by *C. echinulata* FR3 after 6 days.

605 **Figure 4.** Transcriptomic analysis to reveal the lignocellulose degradation mechanisms in *C.*  
606 *echinulata* FR3. (A) Expression abundance of selected cellulases and hemicellulases. (B)  
607 Expression abundance of selected extracellular lignolytic enzymes and Fenton system related  
608 enzymes. (C) Central aromatic compound catabolism pathway in *C. echinulata* FR3. HGD,  
609 homogentisate 1,2-dioxygenase; maiA, maleylacetoacetate isomerase; FAH, fumarylacetoacetase;  
610 HAAO, 3-hydroxyanthranilate 3,4-dioxygenase; ACMSD, aminocarboxymuconate-  
611 semialdehyde decarboxylase.

612 **Figure 5.** An integrated model to elucidate the lignocellulose degradation mechanisms in *C.*  
613 *echinulata* FR3. LMCO, laccase-like multiple copper oxidase; APO, aromatic peroxygenase;  
614 CYP, Cytochrome P450; Cel, cellulase; Hem, hemicellulase; QRD, quinone reductase; FeR,  
615 ferric reductase; GAO, galactose oxidase; GMC, GMC oxidoreductase; QUT, quinate permeases;  
616 ADE, aromatic compound degradation enzymes.

617 **Figure 6.** Measurement of iron-reducing activity of the cultivation supernatant of *C. echinulata*  
618 FR3 grown on wild-type (solid triangle) sorghum biomass, *bmr6/bmr12* double mutant (solid  
619 square) sorghum biomass, and PDB (solid inverted triangle).

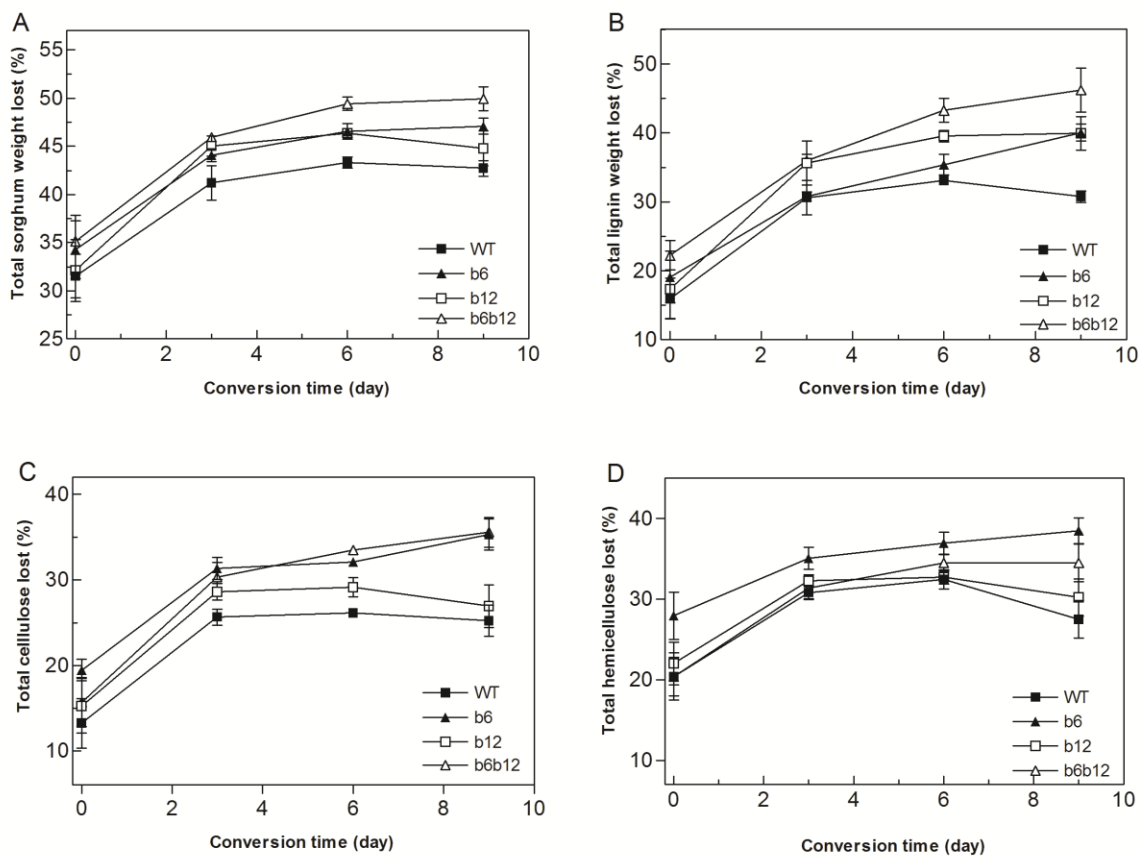
620

<b>Biomass samples</b>	<b>Carbohydrate content (%)</b>	<b>Aromatic content (%)</b>	<b>Methoxyl group (%)</b>	<b>Aliphatic carbonyl/ carboxyl group (%)</b>	<b>Aliphatic carbon content (%)</b>	<b>Carbohydrate/ Aromatic ratio</b>
WT-raw	66.7	16.8	3.3	3.7	6.5	4
WT-6 days	75.4	12.1	2.5	2.7	4.1	6.2
b6b12-raw	63.4	18.6	3.2	5.3	6.2	3.4
b6b12-6 days	73.4	13.0	2.4	3.7	3.9	5.7

621

622

Table 1



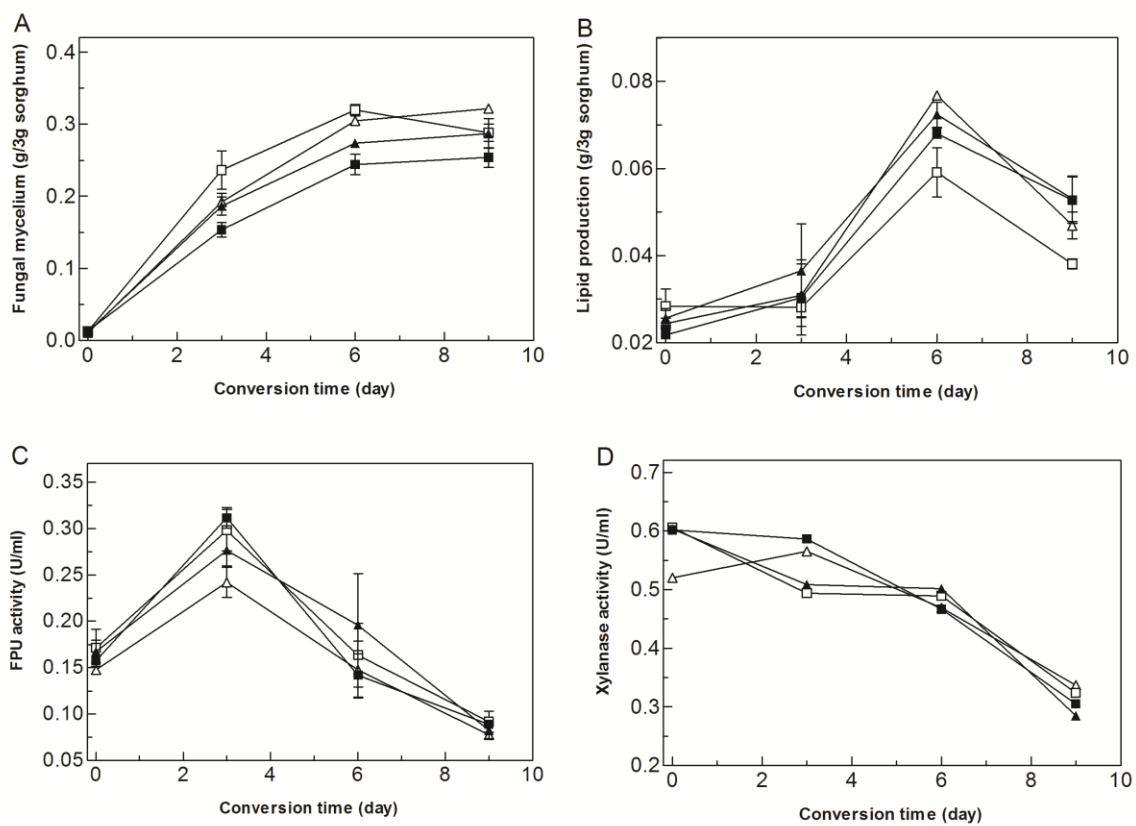
623

624

625

626

Figure 1



627

628

629

Figure 2

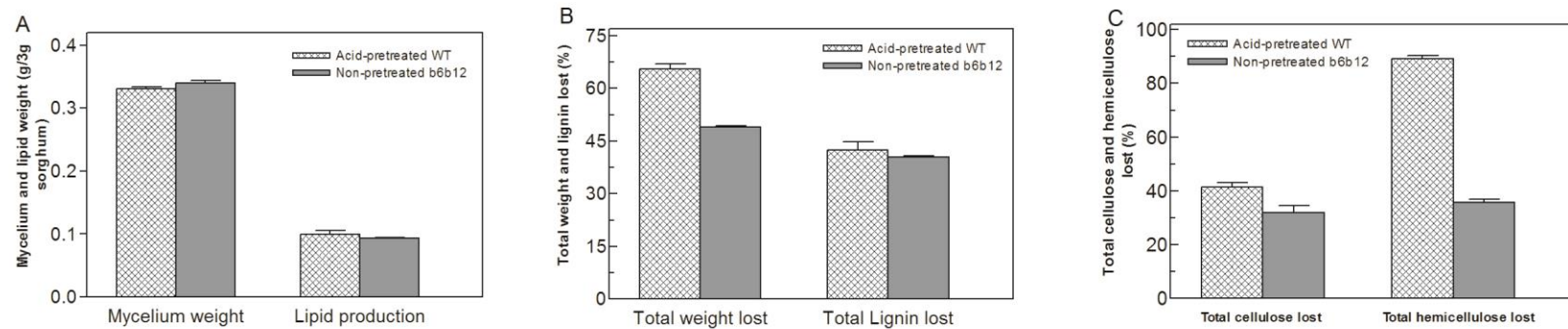
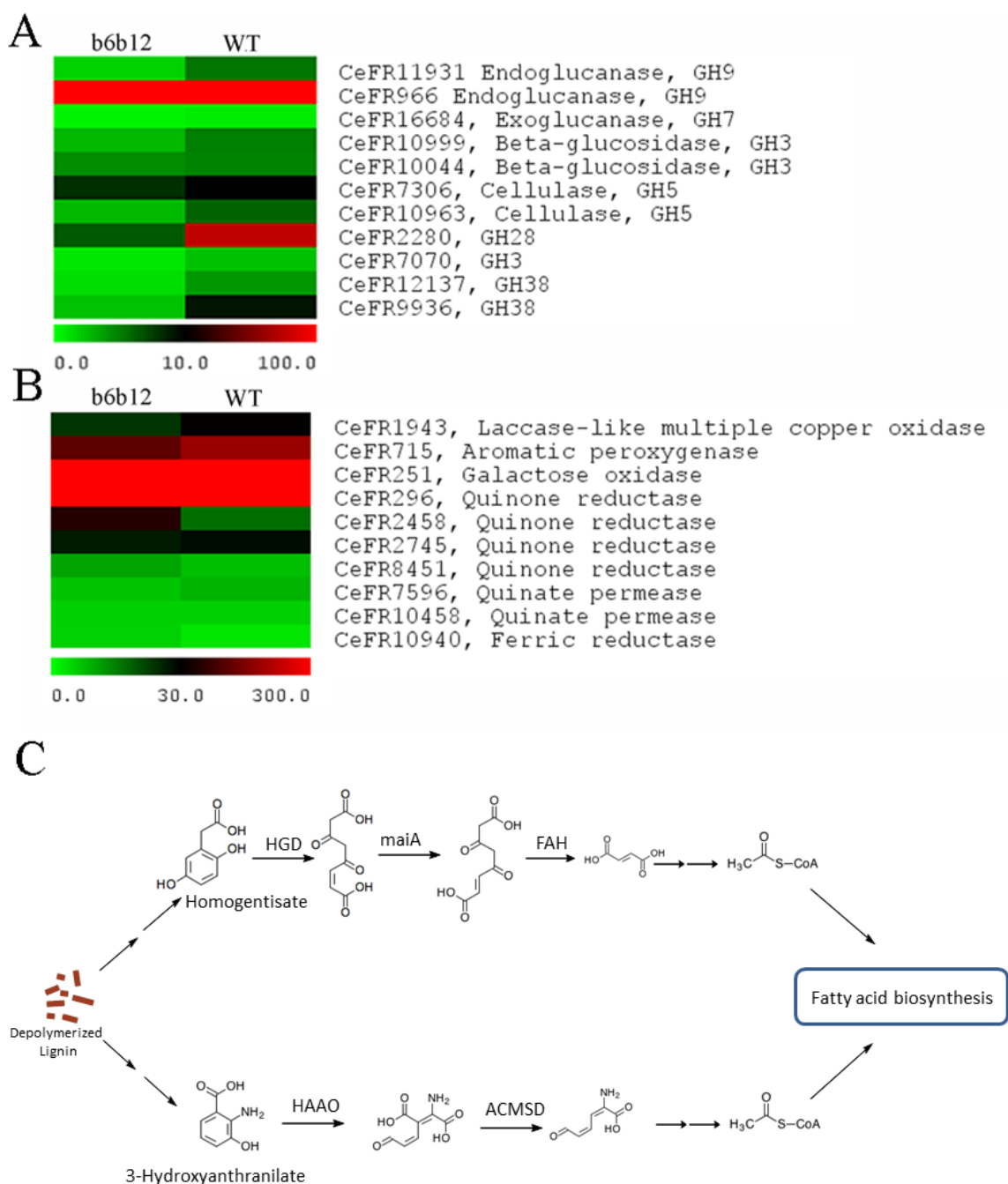


Figure 3

630

631

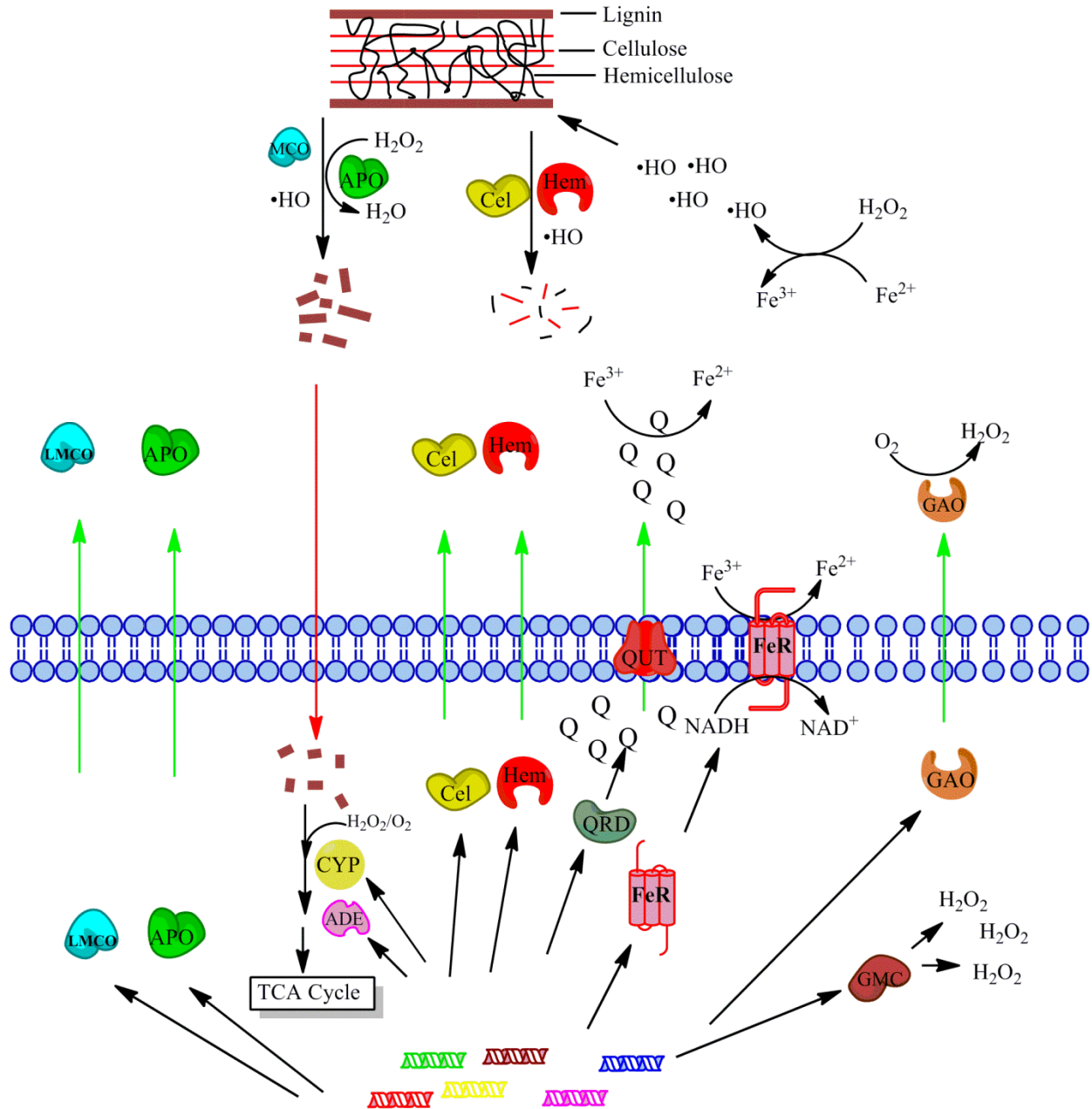


632

633

634

Figure 4



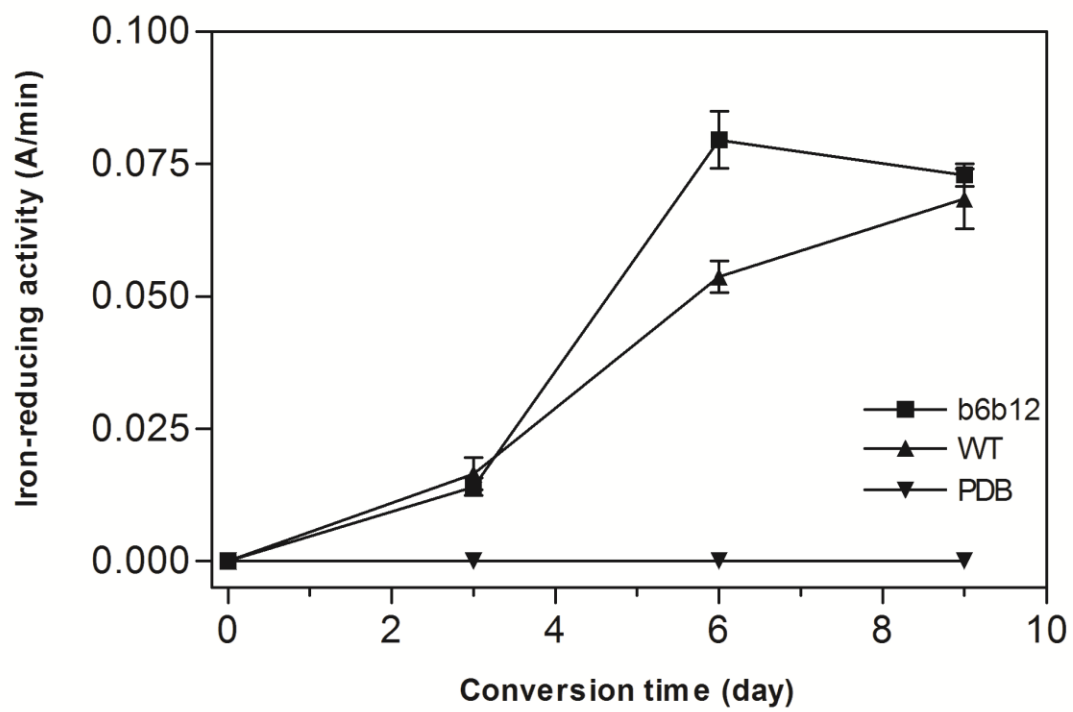
635

636

637

Figure 5

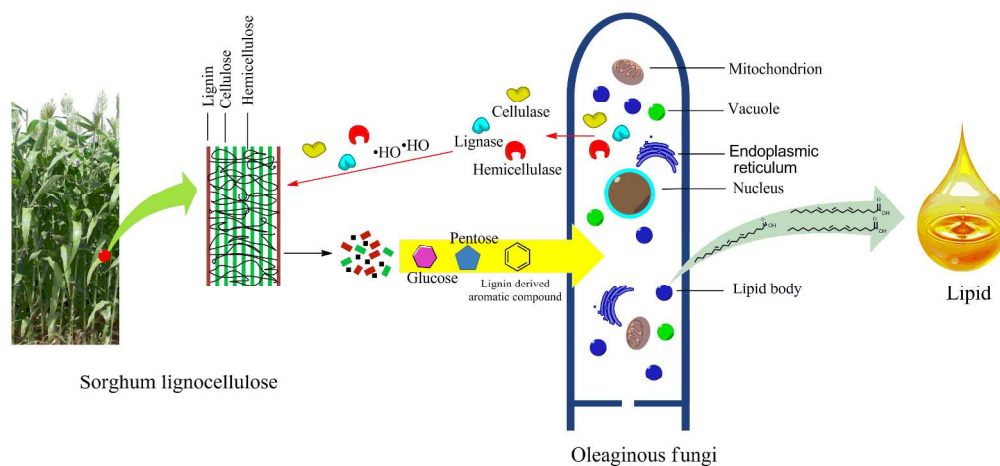




638

639

Figure 6



Biomass conversion of all cell wall components can be achieved by oleaginous fungus *C. echinulata* FR3. The strain represents one of the rare non-basidiomycetes with a strong lignin degradation machinery and capacity to convert all cell wall components to a fungible product, lipid. The unique lignin degradation capacity enables a consolidated platform for converting all cell wall components potentially without chemical-physical pretreatment.

271x124mm (300 x 300 DPI)